JPL PUBLICATIONS 78-43

Analysis of a Suspension System for a Wheel Rolling on a Flat Track

H. McGinness

(NASA-CR-157563) ANALYSIS OF A SUSPENSION SYSTEM FOR A WHEEL ROLLING ON A FLAT TRACK (Jet Propulsion Lab.) 24 p HC A02/MF A01 CSCL 13I
N78-30583
Unclas
G3/37 29112

August 1, 1978

National Aeronautics and
Space Administration

Jet Propulsion Laboratory
California Institute of Technology
Pasadena, California

JPL PUBLICATIONS 78-43

Analysis of a Suspension System for a Wheel Rolling on a Flat Track

H. McGinness

August 1, 1978

National Aeronautics and
Space Administration

Jet Propulsion Laboratory
California Institute of Technology
Pasadena, California

The research described in this publication was carried out by the Jet Propulsion Laboratory, California Institute of Technology, under NASA Contract No. NAS7-100.

ABSTRACT

A flexure strut wheel suspension system is described which keeps a wheel flat against the track and maintains a small interface moment. Equations are presented for the evaluation of this moment. A comparison of the flexure strut system is made with a rigid link design containing pivot bearings.

CONTENTS

Figures

SECTION I

INTRODUCTION

In many engineering applications a roller or uncrowned wheel bears against a flat track. Usually it is desirable that the loading along the contact area, parallel to the wheel axis, be symmetrical and as nearly uniform as possible. If the loading is not symmetrical, an interface moment will exist between the wheel and track, and the effect of the moment is to increase the load intensity at one edge of the wheel and reduce it at the other edge.

A wheel suspension system is described which keeps the wheel flat against the track and limits the interface moment to small values. A method of evaluating the moment is presented.

SECTION II

DESCRIPTION OF THE WHEEL SUSPENSION

The basic configuration of the wheel suspension system is shown in Fig. 2-1. The wheel frame is attached to the base structure by sloping support struts, the ends of which are firmly connected to the wheel frame and base structure. In the ideal position the center planes of the struts intersect the top surface of the track in a line which is also the path of the wheel contact center. In this position the wheel-track contact load distribution is symmetrical about the wheel-track contact center, called the wheel-track origin, and the moment about this point, called the interface moment M_1, is zero. This condition makes the peak contact stresses a minimum, and produces only axial forces in the support struts. This ideal position is represented by the solid line sketch of Fig. 2-2a. If the cross section of the track rotates from its ideal position by the small angle θ_4, as shown by the dashed lines of Fig. 2-2a, the support struts become displaced, as indicated by the dashed lines, and have finite end moments and shears. The reactive moments and shears on the wheel frame, together with the axial load in the displaced strut, sum to form an interface moment, which under special conditions can be zero but is usually finite. In all practical cases the interface moment will be small enough to allow the wheel to remain flat against the track.

The analysis of the support strut as a beam column, as shown in Fig. 2-2b, will give the moment and shear at station 4, where the strut attaches to the wheel frame. In the following analyses all parts except the support struts are considered rigid. Also it is considered that there is only one strut on each side of the wheel, the properties of which are equal to the sum of two or more identical struts on each side. Two types

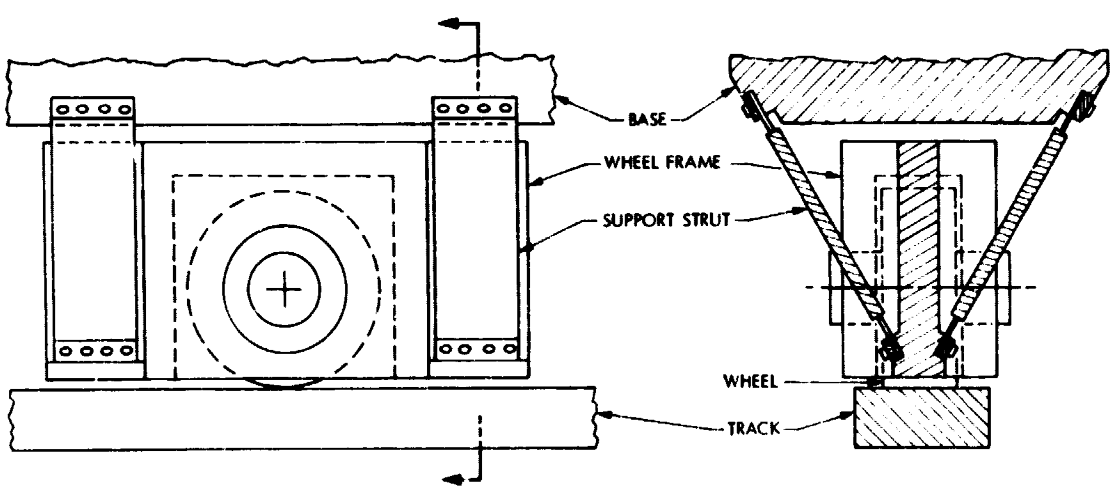

Fig. 2-1. Wheel suspension system

of flexure struts will be analyzed, namely,one of constant cross section of length ℓ, and one composed of end flexures of lengths ℓ_1 and ℓ_4 connected by a rigid member of length m. Both ℓ_1 and ℓ_4 have constant properties over their lengths, but the properties of ℓ_1 may be different from those of ℓ_4.

A third type employing rigid struts with pivot bearings will also be analyzed and compared to the flexure strut system.

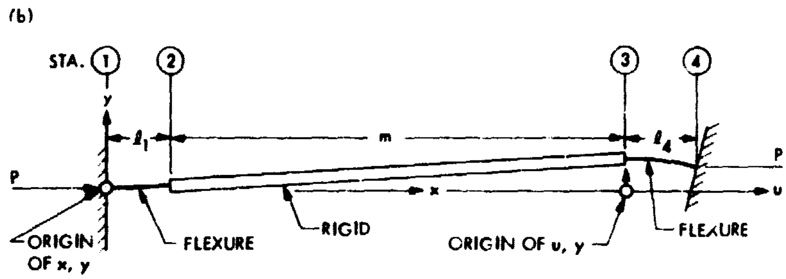

Fig. 2-2b. Cordinate systems

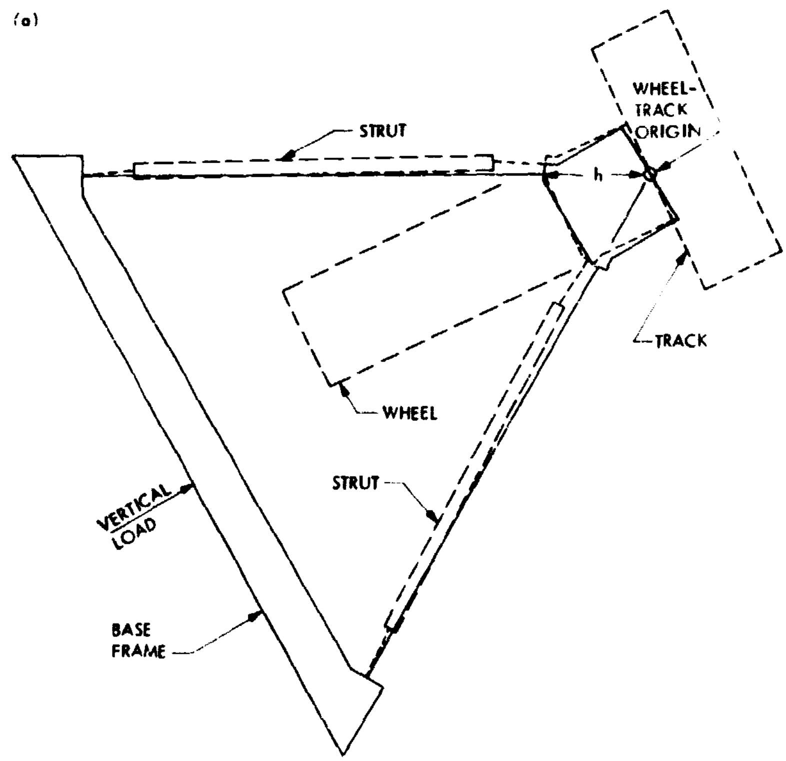

Fig. 2-2a. Schematic diagram of suspension with flexure support struts

SECTION III

BEAM COLUMN EQUATIONS

It is convenient to employ the solutions of the fourth-order differential equation for the cases at hand, which are limited to small deflections and have no transverse forces between the ends of the beam elements. For these conditions the following equation from Ref. 1 applies:

$$\frac{d^4y}{dx^4} + k^2 \frac{d^2y}{dx^2} = 0 \tag{1}$$

where

$$k^2 = P/EI$$

P is the column load

E is the modulus of elasticity

I is moment of inertia of area about the axis perpendicular to the plane of bending of the strut

The general solution of (1) is

$$Y = A \sin kx + B \cos kx + Cx + D \tag{2}$$

where A, B, C, and D are constants to be determined from the end conditions. The slope dy/dx and moment M are obtained by differentiating (2) and are:

$$\frac{dy}{dx} = Ak \cos kx - Bk \sin kx + C \tag{3}$$

$$M = EI \frac{d^2y}{dx^2} = - P(A \sin kx + B \cos kx) \tag{4}$$

The shear S perpendicular to the undeflected beam axis is:

$$S = \frac{dM}{dx} + P\frac{dy}{dx} = CP \tag{5}$$

The constants A, B, C, and D can be determined by applying two proper end conditions to each end of each beam column element. In each case to be considered, the deflection and slope are both zero at the left-hand end of the strut as pictured in Fig. 2-2b, that is, at the origin of the X-axis. At the right-hand end of the strut at $x = \ell$, the slope has the known value θ_4, that is, it is equal to the tilt of the track. With the coordinate system shown in Fig. 2-2b, the value of the right end slope shown is negative. Also the deflection at the right-hand end is y_4, which is related to θ_4 as follows:

$$y_4 = -h\theta_4 \tag{6}$$

where the distance h is shown in Fig. 2-2b.

For the case of a single flexure of length ℓ and of constant cross section, the following equations may be written from (2) and (3):

$$Y_{x=0} = B + D = 0 \tag{7}$$

$$\left.\frac{dy}{dx}\right]_{x=0} = kA + C = 0 \tag{8}$$

$$y_{x=\ell} = (\sin k\ell)\,A + (\cos k\ell)B + \ell C + D = -h\theta_4 \tag{9}$$

$$\left.\frac{dy}{dx}\right]_{x=\ell} = (k\cos k\ell)\,A - (k\sin k\ell)B + C = \theta_4 \tag{10}$$

The characteristic equation of (7), (8), (9), and (10) is:

$$k[2(1 - \cos k\ell) - k\ell\sin k\ell] = 0 \tag{11}$$

The lowest nontrivial value of $k\ell$ satisfying (11) is

$$k\ell = 2\pi \tag{12}$$

Since $k = \sqrt{P/EI}$, the following critical value of the column load, P_{CR}, is obtained:

$$P_{CR} = \frac{4\pi^2 EI}{\ell^2} \tag{13}$$

Solving (7), (8), (9), (10) simultaneously, one obtains

$$\frac{A}{\theta_4} = \frac{- h \sin k\ell - \frac{1}{k}(1 - \cos k\ell)}{2(1 - \cos k\ell) - k\ell \sin k\ell} \tag{14}$$

$$\frac{B}{\theta_4} = \frac{h(1 - \cos k\ell) + \ell - \frac{1}{k}\sin k\ell}{2(1 - \cos k\ell) - k\ell \sin k\ell} \tag{15}$$

$$C = - kA \tag{16}$$

$$D = - B \tag{17}$$

These values of A and B allow the equation for M to be evaluated for any value of X in terms of θ_4. At $x = \ell$, the moment is

$$\frac{M_4}{\theta_4} = \frac{M_{x=\ell}}{\theta_4} = P\left[\frac{h(1 - \cos k\ell) - \ell \cos k\ell + \frac{1}{k}\sin k\ell}{2(1 - \cos k\ell) - k\ell \sin k\ell}\right] \tag{18}$$

From (5), the shear S is constant over the beam length and is

$$\frac{S}{\theta_4} = \frac{-kAP}{\theta_4} = P\left[\frac{kh \sin k\ell + (1 - \cos k\ell)}{2(1 - \cos k\ell) - k\ell \sin k\ell}\right] \tag{19}$$

If the shear is negative, the equilibrating force on the beam at the right-hand end, station 4, acts upward.

Since the forces and moment acting at the right-hand end of the beam are now known, the equal and opposite forces and moment acting on the wheel frame are also known, thus allowing the total moment about the wheel-track origin to be evaluated. This, by definition, is the interface moment being sought.

For the case of the support strut being composed of two flexures separated by a rigid centerpiece of length m, the forces and moment at station 4 of Fig. 2-2b can be determined in a similar but more complicated way. Referring to Fig. 2-2b, the left flexure can be solved in terms of Y_2 and θ_2, the deflection and slope at station 2. Similarly, the right flexure can be solved in terms of Y_3, θ_3, Y_4, θ_4. Making use of relationships between θ_2 and θ_3, and between Y_2 and Y_3, and then employing two different moment equilibrium equations, the unknowns Y_2 and θ_2 can be obtained. Using subscripts 1 and 4 for the left and right flexures, respectively, the following are obtained:

$$Y = A_1 \sin k_1 x + B_1 \cos k_1 x + C_1 x + D \tag{20}$$

Using the boundary conditions

$$Y_{x=0} = 0, \left.\frac{dy}{dx}\right|_{x=0} = 0, Y_{x=\ell_1} = Y_2, \left.\frac{dy}{dx}\right|_{x=\ell_1} = \theta_2$$

the following values of the constants are obtained:

$$A_1 = \frac{(\sin k_1\ell_1)\, Y_2 - \frac{1}{k_1}(1 \cos k_1\ell_1)\,\theta_2}{2(1 - \cos k_1\ell_1) - k_1\ell_1 \sin k_1\ell_1} \tag{21}$$

$$B_1 = \frac{-(1 - \cos k_1\ell_1)\, Y_2 + \left(\ell_1 - \frac{1}{k_1}\sin k_1\ell_1\right)\theta_2}{2(1 - \cos k_1\ell_1) - k_1\ell_1 \sin k_1\ell_1} \tag{22}$$

$$D_1 = - B_1 \tag{23}$$

$$C_1 = - k_1 A_1 \tag{24}$$

The moment M_1 at station 1 is

$$M_1 = M_{x=0} = - P\left[\frac{-(1 - \cos k_1\ell_1)\, Y_2 + \left(\ell_1 - \frac{1}{k_1}\sin k_1\ell_1\right)}{2(1 - \cos k_1\ell_1) - k_1\ell_1 \sin k_1\ell_1}\right] \tag{25}$$

ORIGINAL PAGE IS
OF POOR QUALITY

The shear at X = 0 is

$$S_{x=0} = PC_1 = -P \frac{(k_1 \sin k_1\ell_1)\, Y_2 - (1 - \cos k_1\ell_1)\, \theta_2}{2(1 - \cos k_1\ell_1) - k_1\ell_1 \sin k_1\ell_1} \tag{26}$$

The deflection of the right flexure in terms of coordinate u (see Fig. 2-2b) is

$$Y = A_4 \sin k_4 u + B_4 \cos k_4 u + C_4 u + D_4 \tag{27}$$

Using the boundary conditions

$$Y_{u=0} = Y_3 = Y_2 + m\theta_2$$

$$\left.\frac{dy}{du}\right]_{u=0} = \theta_3 = \theta_2$$

$$Y_{u=\ell_4} = Y_4 = -h\theta_4$$

$$\left.\frac{dy}{du}\right]_{x=\ell_4} = \theta_4 \tag{28}$$

the following values of the constants are obtained:

$$A_4 = \frac{-(\sin k_4\ell_4)\, Y_2 - \left[m(\sin k_4\ell_4) - \frac{1}{k_4}(1 \cos k_4\ell_4 - k_4\ell_4 \sin k_4\ell_4)\right]\theta_2 - \left[h(\sin k_4\ell_4) + \frac{1}{k_4}(1 - \cos k_4\ell_4)\right]\theta_4}{2(1 - \cos k_4\ell_4) - k_4\ell_4 \sin k_4\ell_4} \tag{29}$$

$$B_4 = \frac{(1 - \cos k_4\ell_4)\, Y_2 + \left[m(1 - \cos k_4\ell_4) + \frac{1}{k_4}(\sin k_4\ell_4 - k_4\ell_4 \cos k_4\ell_4)\right]\theta_2 + \left[h(1 - \cos k_4\ell_4) + \frac{1}{k_4}(k_4\ell_4 - \sin k_4\ell_4)\right]\theta_4}{2(1 - \cos k_4\ell_4) - k_4\ell_4 \sin k_4\ell_4} \tag{30}$$

$$D_4 = Y_2 + m\theta_2 - B_4 \tag{31}$$

$$C_4 = \theta_2 - k_4 A_4 \tag{32}$$

The moment at $u = 0$ is

$$M_3 = M_{u=0} = -P \left\{ \frac{(1 - \cos k_4\ell_4)\,Y_2 + \left[m(1 - \cos k_4\ell_4) + \frac{1}{k_4}(\sin k_4\ell_4 - k_4\ell_4 \cos k_4\ell_4)\right]\theta_2 + \left[h(1 - \cos k_4\ell_4) + \frac{1}{k_4}(k_4\ell_4 - \sin k_4\ell_4)\right]\theta_4}{2(1 - \cos k_4\ell_4) - k_4\ell_4 \sin k_4\ell_4} \right\} \tag{33}$$

The moment at $u = \ell_4$ is

$$M_4 = M_{u=\ell_4} = P \left\{ \frac{(1 - \cos k_4\ell_4)\,Y_2 + \left[m(1 - \cos k_4\ell_4) + \frac{1}{k_4}(k_4\ell_4 - \sin k_4\ell_4)\right]\theta_2 + \left[h(1 - \cos k_4\ell_4) - \frac{1}{k_4}(k_4\ell_4 \cos k_4\ell_4 - \sin k_4\ell_4)\right]\theta_4}{2(1 - \cos k_4\ell_4) - k_4\ell_4 \sin k_4\ell_4} \right\} \tag{34}$$

Now consider a free body diagram of the entire strut as shown in Figs. 3-1 and 3-2, and write the moment equilibrium as follows:

$$(m + \ell_1 + \ell_4)S + M_1 - M_4 + Ph\theta_4 = 0 \tag{35}$$

Next consider a free body diagram of the right-hand flexure only, as shown in Fig. 3-3. From Fig. 2-2b, it may be seen that

$$Y_4 - Y_3 = - h\theta_4 - Y_2 - m\theta_2 \tag{36}$$

The moment equilibrium of the right-hand flexure is

$$\ell_4 S + M_3 - M_4 - P(-h\theta_4 - Y_2 - m\theta_2) = 0 \tag{37}$$

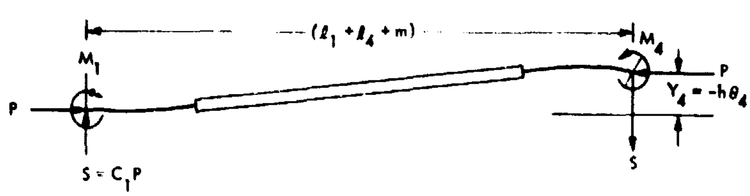

Fig. 3-1. Free body diagram of strut

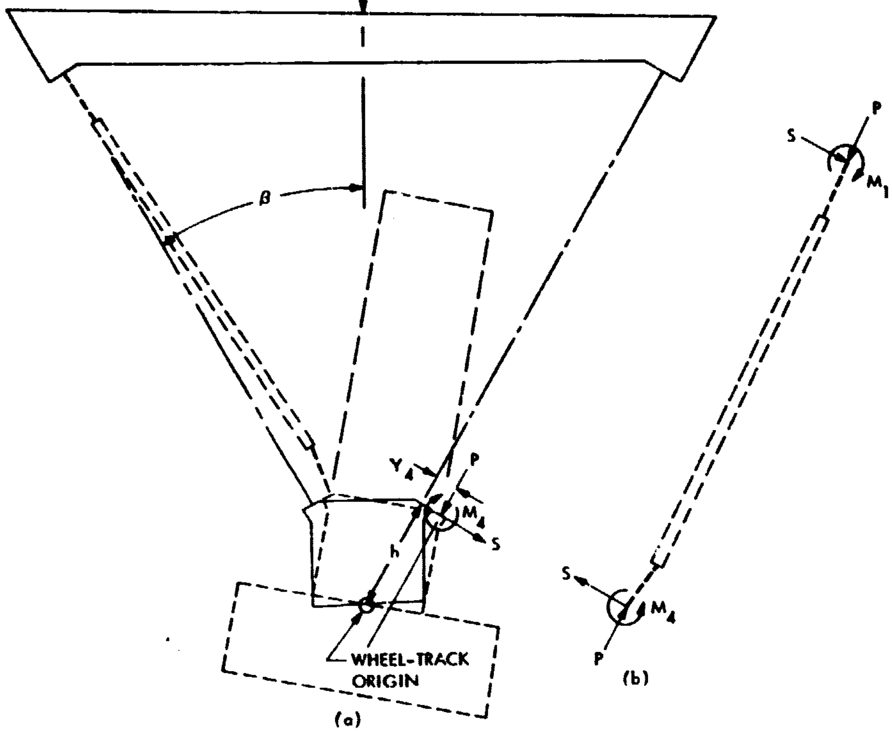

Fig. 3-2. Orientation of free body diagram of flexure strut

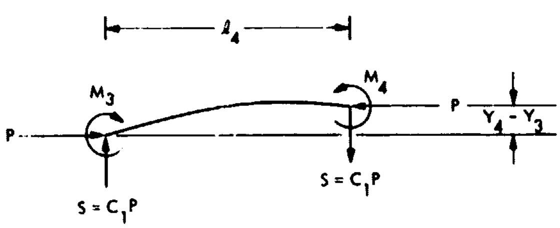

Fig. 3-3. Free body diagram

Substitute (25), (26), (33), and (34) into (35) and (37). This produces two independent equations in the unknowns Y_2 and θ_2 and with the known θ_4 appearing on the right side of the equations as follows:

$$\left[\frac{-(m + \ell_1 + \ell_4)\, k_1 \sin k_1\ell_1 + (1 - \cos k_1\ell_1)}{2(1 - \cos k_1\ell_1) - k_1\ell_1 \sin k_1\ell_1} - \frac{(1 - \cos k_4\ell_4)}{2(1 - \cos k_4\ell_4) - k_4\ell_4 \sin k_4\ell_4}\right] Y_2$$

$$+\left[\frac{(m + \ell_1 + \ell_4)(1 - \cos k_1\ell_1) - \ell_1 + \frac{1}{k_1} \sin k_1\ell_1}{2(1 - \cos k_1\ell_1) - k_1\ell_1 \sin k_1\ell_1} - \frac{m(1 - \cos k_4\ell_4) + \ell_4 - \frac{1}{k_4} \sin k_4\ell_4}{2(1 - \cos k_4\ell_4) - k_4\ell_4 \sin k_4\ell_4}\right] \theta_2$$

$$= \left[\frac{h(1 - \cos k_4\ell_4) - \ell_4 \cos k_4\ell_4 + \frac{1}{k_4} \sin k_4\ell_4}{2(1 - \cos k_4\ell_4) - k_4\ell_4 \sin k_4\ell_4} - h\right] \theta_4 \qquad (38)$$

$$\left[1 - \frac{k_1\ell_4 \sin k_1\ell_1}{2(1 - \cos k_1\ell_1) - k_1\ell_1 \sin k_1\ell_1} - \frac{2(1 - \cos k_4\ell_4)}{2(1 - \cos k_4\ell_4) - k_4\ell_4 \sin k_4\ell_4}\right] Y_2$$

$$+\left[m + \frac{\ell_4(1 - \cos k_1\ell_1)}{2(1 - \cos k_1\ell_1) - k_1\ell_1 \sin k_1\ell_1} - \frac{(2m + \ell_4)(1 - \cos k_4\ell_4)}{2(1 - \cos k_4\ell_4) - k_4\ell_4 \sin k_4\ell_4}\right] \theta_2$$

$$= \left[\frac{(2h + \ell_4)(1 - \cos k_4\ell_4)}{2(1 - \cos k_4\ell_4) - k_4\ell_4 \sin k_4\ell_4} - h\right] \theta_4 \qquad (39)$$

ORIGINAL PAGE IS
OF POOR QUALITY

When Y_2 and θ_2 have been evaluated from solving (38) and (39) simultaneously, M_4 can be obtained from (34), and S is

$$S = PC_1 = - Pk_1A_1 \tag{40}$$

Substituting (21) into (40) results in

$$S = - P\left[\frac{k_1(\sin k_1\ell_1)\ Y_2 - (1 - \cos k_1\ell_1)\theta_2}{2(1 - \cos k_1\ell_1) - k_1\ell_1 \sin k_1\ell_1}\right] \tag{41}$$

In Fig. 3-2b, a free body diagram of the support strut is shown with the forces P and S and the moment M_4 acting on the end which joins the wheel frame. Figure 3-2a shows the equal and opposite forces and moment applied to the wheel frame. The clockwise moment about the wheel-track origin produced by both struts, and defined as the interface moment, is

$$M_i = 2[M_4 + PY_4 + hS] \tag{42}$$

Figure 2-2a shows that $Y_4 = -h\theta_4$; thus (42) becomes

$$M_i = 2[M_4 - Ph\theta_4 + hS] \tag{43}$$

Equation (43) applies to either the double-flexure strut or the single-flexure strut. For the former case, Y_2 and θ_2 must be obtained by solving (38) and (39) simultaneously, evaluating M_4 from (34) and S from (26). For the case of the single flexure, Eq. (18) and (19) can be substituted into (43), yielding

$$\left[\frac{M_i}{\theta_4}\right]_{\substack{\text{single}\\ \text{flexure}}} = 2P\left[\frac{\frac{1}{k} + kh^2 + k\ell h)\sin k\ell - \ell \cos k\ell}{2(1 - \cos k\ell) - k\ell \sin k\ell}\right] \tag{44}$$

Since it is possible for the numerator of the right side of (44) to be zero, the interface moment can be zero.

The effect of the interface moment on the wheel-track loading intensity, for the case when the wheel is flat against the track, can be approximated by assuming that the interface moment is equilibrated by a triangularly distributed load between the wheel and track. Let w_1 be the maximum intensity of the triangularly distributed load. The usual relationship between w_1 and M_i is

$$w_1 = \frac{6M_i}{L^2} \tag{45}$$

where L is the width of the wheel.

Let w_2 be the rectangularly distributed loading between the wheel and track caused by the total vertical load W acting on the wheel.

$$w_2 = \frac{W}{L} \tag{46}$$

The maximum loading intensity w_{max} is the sum of w_2 and the absolute value of w_1, namely,

$$w_{max} = w_2 + |w_1| \tag{47}$$

From Fig. 3-2 it is clear that

$$P = \frac{W}{2 \cos \beta} \tag{48}$$

If (48) is substituted into (44) and the result substituted into (47),

$$w_{max} = \frac{W}{L} \left\{ 1 + \left| \frac{6\theta_4}{L \cos \beta} \left[\frac{\left(\frac{1}{k} + kh^2 + k\ell h \right) \sin k\ell - \ell \cos k\ell}{2(1 - \cos k\ell) - k\ell \sin k\ell} \right] \right| \right\} \tag{49}$$

In this form the effect of the interface moment (of the single flexure configuration) on the contact load intensity can easily be compared to unity, which is the intensity loading factor when the interface moment is zero.

SECTION IV

CRITICAL COLUMN LOADS

The critical column load P_{CR} is the column load that produces instability or buckling regardless of the magnitude of compressive and/or bending stresses in the beam column. Its value is determined by end conditions which remain constant as the column load increases. The single-flexure critical load is given by Eq. (13) and was derived by considering the slopes and deflections to be fixed at both ends.

The critical load for the general case of two different end flexures will not be discussed. However, the special case of the two end flexures being identical has a simple solution. From symmetry, it would be expected that the slope of the rigid connecting member would remain constant. The shear is also constant over the entire length of the strut. Therefore, at the end of the flexure which joins the rigid connecting member, the proper end conditions are constant slope and constant shear. At the other end of the flexure, the two end conditions are constant deflection and constant slope. The characteristic equation is formed by applying Eqs. (2) and (3) at, say, the left end, where $X = 0$, and Eqs. (3) and (5) at the right end, where $X = \ell_2$. The resulting characteristic equation is

$$Pk_1^2 \sin k_1\ell_1 = 0 \tag{50}$$

The lowest nontrivial value of $k_1\ell_1$ is π; hence

$$P_{\substack{CR\\ \text{DOUBLE}\\ \text{FLEXURE}}} = \frac{\pi^2 EI}{\ell_1^2} \tag{51}$$

SECTION V

SUSPENSION SYSTEM WITH PIVOT BEARINGS

Figure 5-1a shows another wheel suspension system consisting of sloping rigid links connecting the base frame to the wheel frame. The link ends are pivoted in bearings. The ideal configuration is shown in solid lines, and the tilted track configuration is shown by dashed lines.

From Fig. 5-1a, it may be seen that the lower pivot is displaced from its ideal position by an amount $h\theta$. The moment arm that the dashed link has with the origin is $[h\theta(\ell + h)/\ell]$. Letting P be the nominal axial load in one link, the clockwise moment about the origin M_p is

$$M_p = P\theta \frac{h}{\ell} (\ell + h) \tag{52}$$

Now consider the equilibrium of the right-hand link as the track tilts so as to increase the value of θ. The frictional moments have the direction and magnitude shown in Fig. 5-1b, where r is the effective radius of the bearing and μ is the friction coefficient. The equilibrating lateral forces R have the directions and magnitude shown in Fig. 5-1b. The equal and opposite forces and moments to the wheel frame are shown in Fig. 5-2.

Referring to Fig. 7, the clockwise interface moment about the origin $\mathcal{M}_i$ is

$$\mathcal{M}_i = 2\left[P\theta \frac{h}{\ell} (\ell + h) - hR - M_F\right] \tag{53}$$

Substituting the expressions for R and M_F shown in Fig. 5-1 results in

$$\mathcal{M}_i = 2P\left[\theta \frac{h}{\ell} (h + \ell) - r\mu \left(1 + 2 \frac{h}{\ell}\right)\right] \tag{54}$$

The negative sign in (54) pertains only when the absolute value of θ as shown in Fig. 5-1a is increasing. If the position is as shown in Fig. 5-1a and the movement is toward the ideal position, the negative sign of (54) becomes positive because the frictional moments act against the direction of movement. Therefore the maximum absolute value of the interface moment $|\mathcal{M}_i|$ may be expressed as

$$|\mathcal{M}_i| = 2P \left[|\theta| \frac{h}{\ell} (h + \ell) + r\mu \left(1 + 2 \frac{h}{\ell}\right)\right] \tag{55}$$

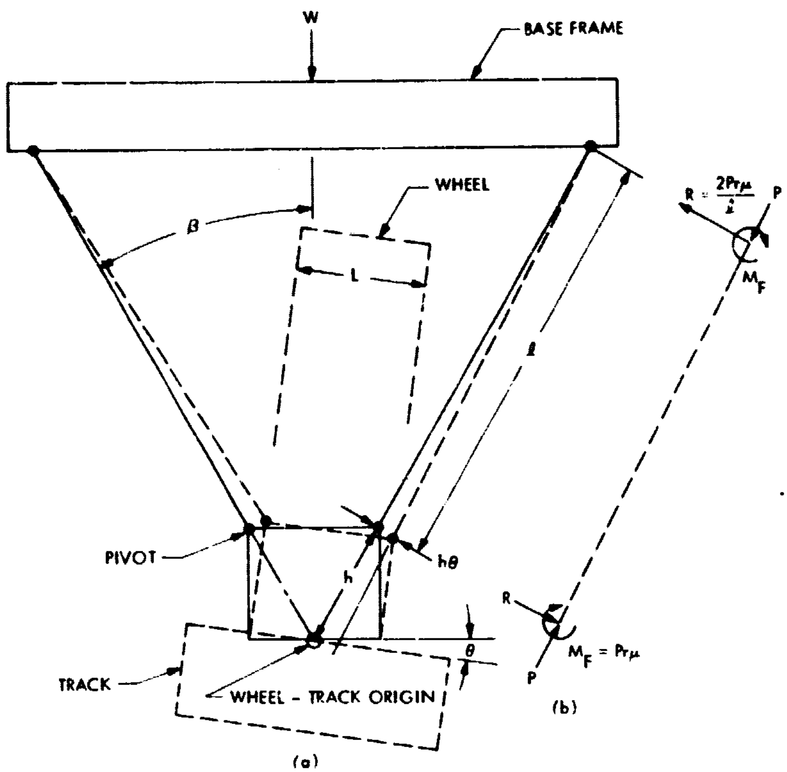

Fig. 5-1. Schematic diagram of suspension system with pivot bearings

Equation (55), in contrast to (44), can have no cancellation of terms. Even a frictionless bearing produces a finite interface moment, whereas it is possible for the flexure system interface moment to be zero.

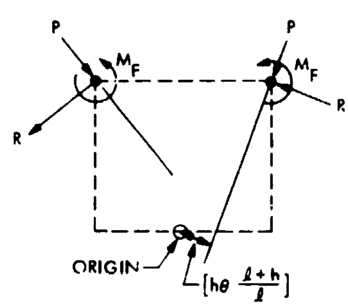

Fig. 5-2. Free body diagram of wheel frame

SECTION VI

EXAMPLES

The following examples, taken from engineering designs of suspension systems for the azimuth bearing of a large antenna, show a typical difference between the pivot bearing and flexure types.

For the pivot bearing type, let $L = 10$, $\cos \beta = 0.866$, $|\theta| = 0.004$ rad, $h = 13$, $\ell = 40$, $r = 3$, $\mu = 0.10$. When these values are substituted into Eq. (55) and the result is used in (47), the following is obtained:

$$w_{max} = \frac{W}{L}\left\{1 + \frac{6}{10(0.866)}\left[0.004\left(\frac{13}{40}\right)53 + 3(0.10)\left(1 + 2 \times \frac{13}{40}\right)\right]\right\}$$

$$= \frac{W}{L}\{1 + 0.391\} \tag{56}$$

which shows that the maximum wheel-track loading intensity is increased by 39% over the ideal value. If the bearing friction coefficient is increased to 0.30, the 39% would increase to 108%, more than twice the ideal value.

For the single-flexure type, let $L = 10$, $\cos \beta = 0.866$, $\theta_4 = 0.004$ rad, $h = 10$, $\ell = 49$, $k = 0.068$. When these values are substituted into Eq. (49),

$$w_{max} = \frac{W}{L}\{1 + |0.0115|\}$$

which shows that the maximum wheel-track loading intensity is increased by only 1.15% over the ideal value.

REFERENCE

1. Sechler, E. E., Elasticity in Engineering, John Wiley and Sons, 1952.